

# USE OF CONTRAST-ENHANCED COMPUTED TOMOGRAPHY TO ASSESS ANGIOGENESIS IN DEEP DIGITAL FLEXOR TENDONOPATHY IN A HORSE

SARAH M. PUCHALSKI, LARRY D. GALUPPO, CLIFTON P. DREW, ERIK R. WISNER

**We compared contrast-enhanced computed tomography (CT) and high field magnetic resonance (MR) imaging in a horse with deep digital flexor tendonopathy. Lesions in the distal extremity were documented grossly and histopathologically. In contrast-enhanced CT, the deep digital flexor tendon lesions were markedly contrast enhancing with evidence of angiogenesis in the core and dorsal border lesions. The lesion morphology was clearly delineated on MR imaging, but without contrast media angiogenesis cannot be identified. Gross examination, histopathologic examination, and CD31 immunohistochemistry confirmed the tendonopathy and an increased presence of small blood vessels. In this horse, deep digital flexor tendon lesions appeared similarly on contrast-enhanced CT and MR imaging. Contrast-enhanced CT may be an alternative to MR imaging for assessing tendon and ligament injury in the digit of the horse. *Veterinary Radiology & Ultrasound*, Vol. 50, No. 3, 2009, pp 292–297.**

**Key words:** angiogenesis, contrast-enhanced CT, equine deep digital flexor tendon, foot, MRI, tendonopathy.

## Introduction

FOOT LAMENESS IS A common cause of loss of use in the equine industry.<sup>1–3</sup> Radiography and ultrasound are limited in their ability to provide a complete evaluation of heel pain, particularly with respect to soft tissue injuries within the hoof capsule.<sup>3,4</sup> Magnetic resonance (MR) imaging allows assessment of soft tissues within the hoof capsule and findings have been associated with histopathologic abnormalities.<sup>5–10</sup> Computed tomography (CT) is also useful for evaluation of bone and soft tissue abnormalities within the foot.<sup>11–13</sup> Contrast-enhanced CT has been proposed as a means of evaluating osseous and soft tissue structures of the foot for diagnosing the cause of heel pain.<sup>14,15</sup>

Anatomic and physiologic changes are expected after tendon injury.<sup>16</sup> Most clinical imaging studies are limited to anatomic characterization of the injury and do not adequately portray ongoing physiologic events. In power Doppler ultrasound studies, an increased number of small blood vessels have been identified leading to increased blood flow in tendinosis of the human patellar and Achilles tendons<sup>17–19</sup> and in injuries of the equine suspensory ligaments and superficial digital flexor tendons.<sup>20</sup> Using

dynamic contrast-enhanced MR imaging, an association between early contrast enhancement and histopathologic abnormalities and pain has been found in human Achilles tendons.<sup>21</sup> Serial examinations of hyperemia and new vessel formation identified using power Doppler may be a method of monitoring tendon healing.<sup>18</sup> In the equine foot, conventional MR imaging is capable of reliably identifying tendon lesions<sup>5,9,10</sup> but has more limited utility in evaluating tendon healing or lesion progression.<sup>22,23</sup> Herein our study describes contrast-enhanced CT findings along with MR imaging, gross and histopathologic abnormalities in a horse with deep digital flexor tendonopathy.

## Materials and Methods

A 6-year-old Oldenburg mare had a 3-month history of right forelimb lameness. Radiographs of both distal extremities were obtained. After radiography, the horse was anesthetized and placed in right lateral recumbency with the right forelimb in the center of a CT scanner gantry.\* A catheter was placed in the medial palmar artery using ultrasound† guidance.<sup>15</sup> Before contrast medium administration, contiguous 3 mm collimated helical images of the foot were acquired. Images were reconstructed using both a bone algorithm and a standard or soft tissue algorithm. An additional examination consisting of 1 mm images was acquired through the navicular bone and distal portion of the deep digital flexor tendon; these were reconstructed using a bone algorithm. A dynamic contrast-enhanced CT study was performed at the level of the most abnormal portion of the deep digital flexor tendon. This study consisted of a

From the Department of Surgical and Radiological Sciences, (Puchalski, Galuppo, Wisner) and the Department of Pathology, Microbiology and Immunology, (Drew), School of Veterinary Medicine, University of California Davis, Davis, CA 95616.

Funding provided by the Center for Equine Health, UC Davis. The Center for Equine Health is supported with funds provided by the Oak Tree Racing Association, The State of California Pari-Mutuel Fund and contributions by private donors.

Address correspondence and reprint requests to Sarah M. Puchalski, at the above address. E-mail: smpuchalski@ucdavis.edu

Received June 9, 2008; accepted for publication November 24, 2008.

doi: 10.1111/j.1740-8261.2009.01536.x

\*HiSpeed FX/I, GE Medical Systems, Milwaukee, WI.

†ATL 5000, Phillips Medical Systems, Bothell, WA.

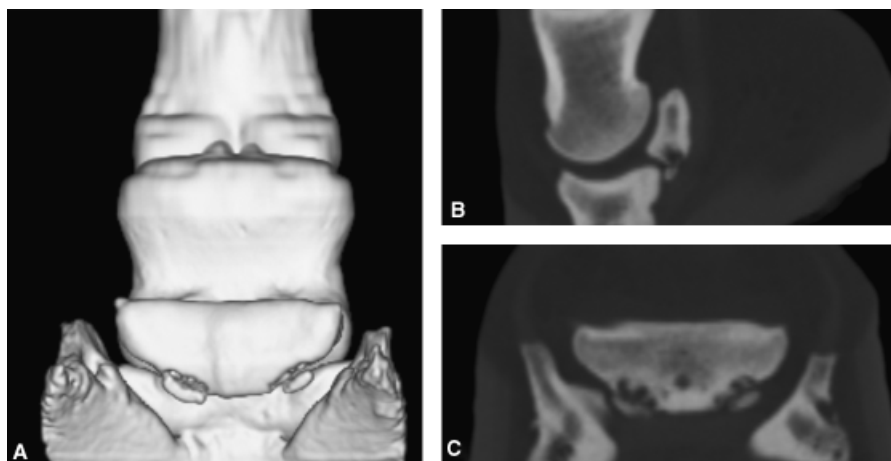


FIG. 1. (A) Three dimensional surface rendering of the distal extremity using the computed tomography images. (B) Sagittal plane and (C) dorsal plane reformatted images. Note the distal navicular bone border fragmentation, increased size of synovial invaginations and proximal border enthesophytosis.

repeated 10 mm collimated image acquired every other second for 90 s before, during, and after administration of ionic-iodinated contrast medium<sup>‡</sup> diluted 1:1 with normal saline into the medial palmar artery. The image acquisition began approximately 5 s before the infusion of contrast medium and continued for 20 s. The image acquisition continued for approximately 65 s to observe temporal changes in enhancement, including venous and tissue contrast medium wash out. The final sequence was a repeat of the first study but acquired during continuous arterial infusion using the same iodinated contrast medium solution. In this sequence, the arterial infusion started approximately 5 s before the onset of image acquisition and continued through the duration of the scan. The presence or absence of contrast medium was identified by subjective visual assessment and the measurement of attenuation in Hounsfield unit using an operator defined, region of interest.

Based on the severity of the disease and the chronic lameness, the horse underwent euthanasia. Immediately before euthanasia, 3 weeks after the initial CT examination, the contrast-enhanced CT examination was repeated. After euthanasia, the right forelimb was disarticulated at the antebrachialcarpal joint and imaged using 1.5 T MR scanner.§ Spin echo T1-weighted, fast spin echo T2-weighted, and gradient recalled echo T2\*-weighted images were acquired in sagittal and transverse planes. A short tau inversion recovery (STIR) sequence was acquired in a sagittal plane. All images had either 3.0 or 3.5 mm slice thickness with a 0.5 mm interslice gap.

After MR imaging, a precision band saw¶ was used to slice the distal limb into 5 mm thick transverse sections the

same plane as the MR and CT images. Histopathologic examination was performed on hematoxylin and eosin-stained 5- $\mu$ m-thick sections. Immunohistochemistry was also performed on select tissue sections, staining for CD31,|| an endothelial cell surface adhesion molecule, thereby allowing identification of small blood vessels.

### Results

Radiographically, typical navicular bone degenerative findings of an increase in size and number of synovial invaginations along the distal navicular border, enthesophyte formation along the extremities of the proximal border, and fragmentation at the proximal attachment of the lateral and medial aspects of the distal sesamoidean impar ligament were found. The sagittal eminence was blunted and the corticomedullary junction poorly defined. In initial CT images these same changes were apparent (Fig. 1A and B). Additionally, in the precontrast CT images a clearly demarcated core lesion that extended to the dorsal border was identified in the medial lobe of the deep digital flexor tendon (Fig. 2A). It extended from approximately 1 cm proximal to the navicular bone distally over the flexor cortex where it became smaller and involved the length of the distal deep digital flexor tendon to its insertion on the distal phalanx. The collateral sesamoidean ligament appeared rounded, mildly heterogenous, and enlarged. During and after intraarterial contrast medium infusion, the lesion of the medial lobe was markedly, centrally contrast enhancing (Fig. 2B). Further contrast enhancement was identified in the dorsal border of the lateral lobe of the deep digital flexor tendon and in the enlarged collateral sesamoidean ligament. Small caliber blood vessels were identified extending into the dorsal border of the deep digital flexor

<sup>‡</sup>RenoCal-76, (400 mg of iodine/ml) Bracco Diagnostics, Princeton, NJ.

<sup>§</sup>Signa LX1.5T, GE Medical System.

<sup>¶</sup>Exakt Cutting/Grinding System, Exakt Technologies Inc., Oklahoma City, OK.

<sup>||</sup>PECAM-1, Santa Cruz Biotechnology Inc., Santa Cruz, CA.

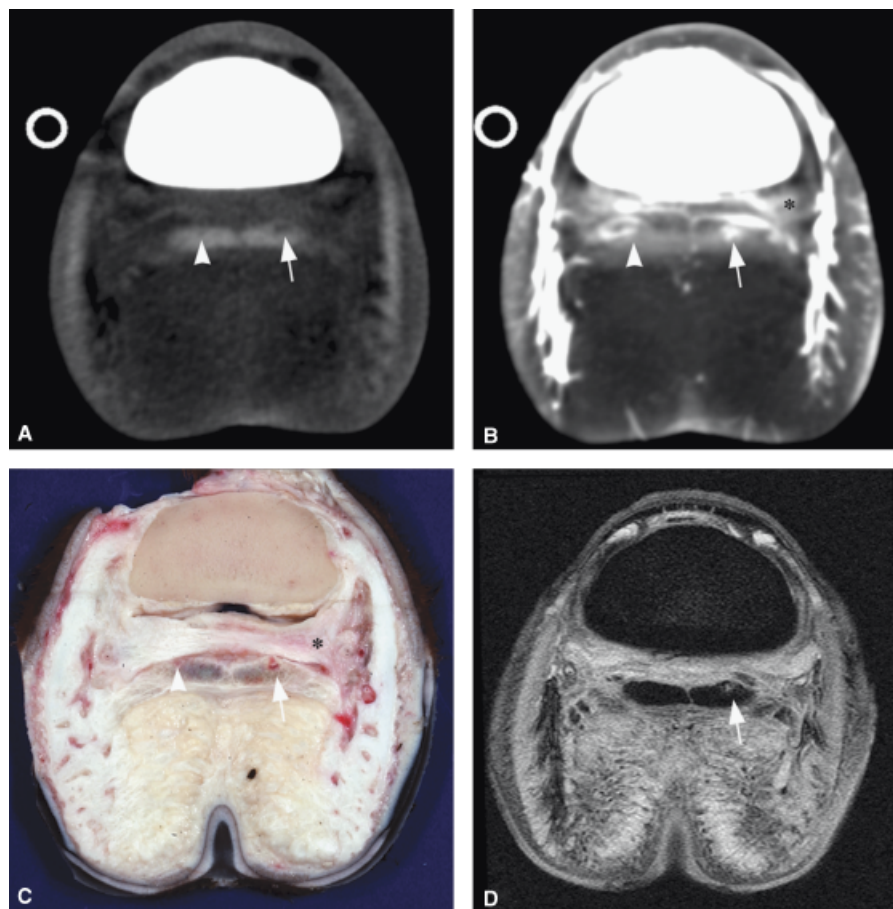


FIG. 2. Transverse images of the distal extremity at the distal aspect of the second phalanx. (A) computed tomography (CT) image, (B) contrast-enhanced CT image, (C) gross specimen, (D) T2\*-weighted, gradient-recalled echo magnetic resonance (MR) image. Note the gross specimen is slightly more distal than the CT and MR images. For all images, lateral is to the left. There is a core lesion of the medial lobe of the deep digital flexor tendon that extends to the dorsal border (arrow). It is clearly identified on all images. There is also an irregular margin of the lateral lobe of the deep digital flexor tendon (arrowhead). On the contrast-enhanced CT images (B) the lesions are more readily identified and relate with the regions of hyperemia seen grossly (C). Note that the lateral collateral sesamoidean ligament (\*) is hyperemic grossly and enhancing on contrast-enhanced CT images. On the MR image (D), the collateral sesamoidean ligaments are present lateral and medial to the distal aspect of the middle phalanx.

tendon (Fig. 2B). Findings of the contrast-enhanced CT examination performed immediately before euthanasia were similar to the first, with minor alterations in the contrast enhancing pattern of the deep digital flexor tendon. As the deep digital flexor tendon lesion extended distally, it coursed to the dorsal border of the tendon lobe where a more peripheral pattern of contrast enhancement was seen (Fig. 3).

In the dynamic contrast-enhanced CT examination at the level of the deep digital flexor tendon lesion, there was contrast enhancement within small blood vessels one image or 1 s after contrast medium was first identified in the regional arteries. The small blood vessels extended from the subsynovial tissues deep to the navicular bursa and entered the dorsal border of deep digital flexor tendon lesion. Contrast medium persisted in the central, previously hypopattenuating lesion of the deep digital flexor tendon until the end of the 90 s acquisition, approximately 10 s after

contrast medium was last seen in regional veins. Contrast medium also persisted within peritendinous tissues.

In MR images the hyperintense core to dorsal border lesion of the medial lobe of the deep digital flexor tendon was clearly seen. The dorsal border of the lateral lobe of the deep digital flexor tendon was irregular (Fig. 2). Navicular bone enthesophyte formation, distal border fragmentation, and enlarged synovial invaginations were also identified. There was medullary hyperintensity within the navicular bone in STIR images. The shallow depression of the distal aspect of the middle phalanx was confirmed with no evidence of associated hyperintensity.

Grossly, the lesion of the deep digital flexor tendon and surrounding soft tissues was characterized by a mottled, white to pale-tan tissue, often surrounded or dissected by thin (<1 mm) bands of red tissue (Fig. 2). Histopathologic examination confirmed the extent, character and distribution of the lesions seen in images of the deep digital

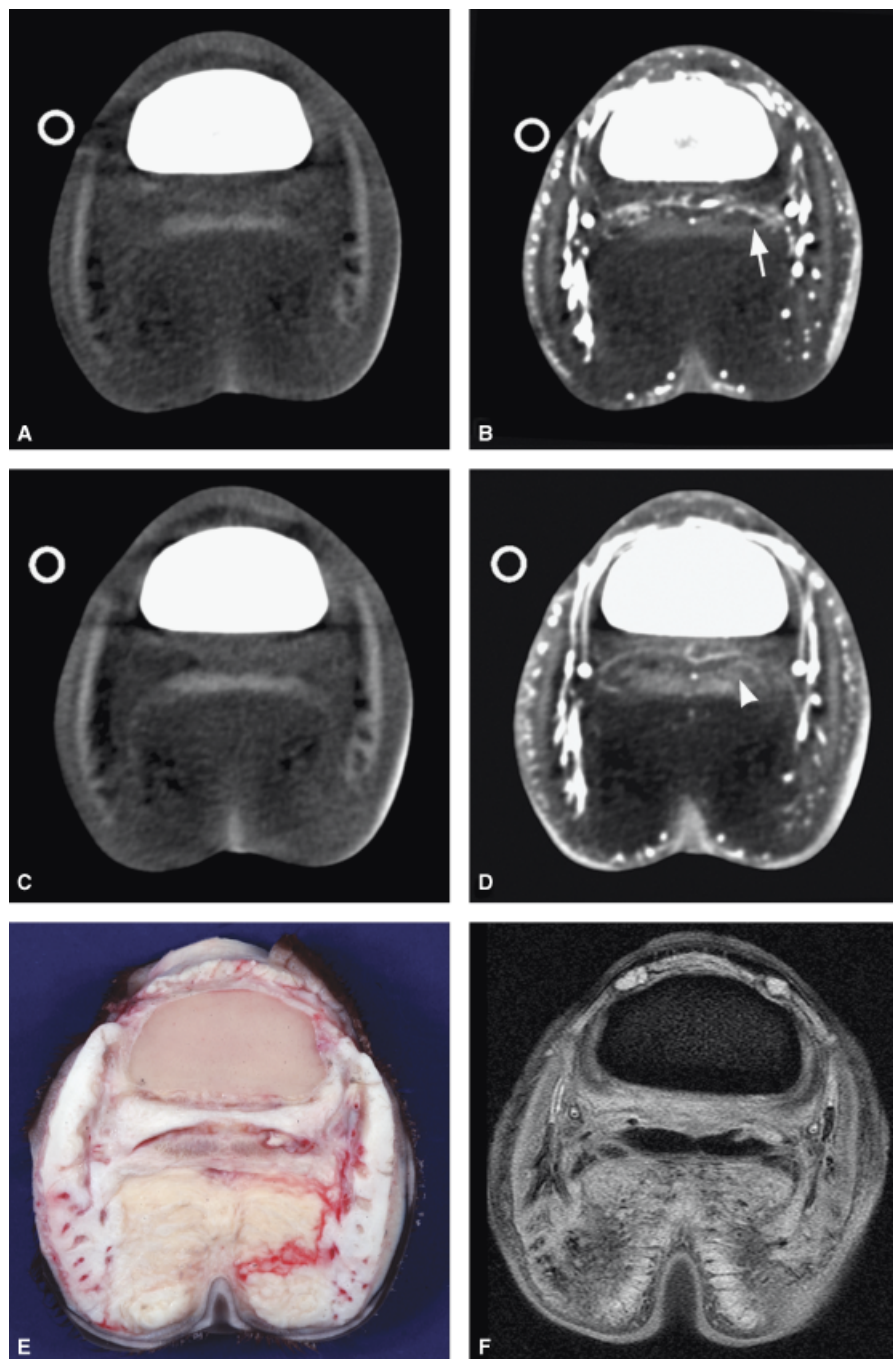


FIG. 3. Transverse images of the distal extremity through distal aspect of the middle phalanx, just proximal to the navicular bone. (A) and (B) Images obtained at the time of the initial examination. (C) and (D) Images obtained on the second contrast-enhanced computed tomography (CT) examination at a similar time to the gross image (E) and the T2\*-weighted gradient-recalled echo magnetic resonance image (F). In the contrast-enhanced CT images (B, D) and the gross image, there is a dorsal border lesion in the medial lobe of the deep digital flexor tendon that has a peripheral rim of contrast enhancement that correlates to a region of tissue hyperemia (arrow). At the earlier time point, the central portion of this lesion does not enhance indicating poor blood supply. At the later time point (D) there is mild enhancement indicating vascular in-growth (arrowhead).

flexor tendon, collateral sesamoidean ligament, and peritendinous soft tissue. The deep digital flexor tendon lesions were characterized by large numbers of densely packed, small caliber vessels that resided on mostly mature fibrous tissue (mature granulation tissue) that replaced, separated,

or expanded the normal tendon fiber bundles with variable extension into adjacent, subsynovial (navicular bursa) tissues (Fig. 4). The peritendinous, subsynovial soft tissues and collateral sesamoidean ligament lesions were characterized by mature, poorly vascularized fibrous tissue that often

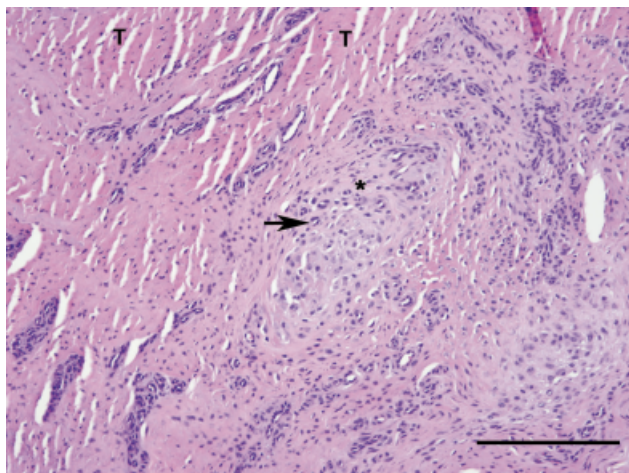


FIG. 4. Photomicrograph of formalin fixed deep digital flexor tendon. Notice that the more normal deep digital flexor tendon fibers (T) are separated by pale matrix (\*) with numerous profiles of small vessels (arrow). Hematoxylin and eosin stain; scale bar = 200  $\mu$ m.

exhibited mucinous degeneration. The subsynovial connective tissue, palmar to the navicular bursa and adjacent to the most severe dorsal deep digital flexor tendon lesions, were expanded by a sparsely cellular, homogeneous collagenous matrix that sent thick fronds of synovial-lined tissue into the synovial space of the navicular bursa. Large aggregates of hemosiderin laden macrophages were common within the subsynovial connective tissue and, to a lesser extent, associated with the fibrous lesions of the deep digital flexor tendon and collateral sesamoidean ligament. Immunohistochemical staining for CD31 confirmed the presence of increased numbers of small caliber, endothelial-lined vessels within the lesions, particularly within the deep digital flexor tendon (Fig. 5).

### Discussion

In this horse, contrast-enhanced CT allowed accurate depiction of the deep digital flexor tendon lesions as compared with histopathologic examination and MR imaging. The dynamic contrast-enhanced CT study allowed further characterization of the tendon lesions, increasing their conspicuity and providing evidence of increased neovessel density and blood flow.

Iodinated contrast media, as used in this horse, are generally small molecular weight substances that mix rapidly in plasma when administered intravascularly. They ultimately distribute to the interstitial space similar to other small molecules, while only a very small percentage enters into the intracellular space (1–2%).<sup>24,25</sup> In inflammatory and neoplastic lesions, increases in perfusion and vascular permeability are expected<sup>26</sup> resulting in an overall increase in the concentration of iodine present or retained in the tissue. Postcontrast CT images are evaluated for changes in

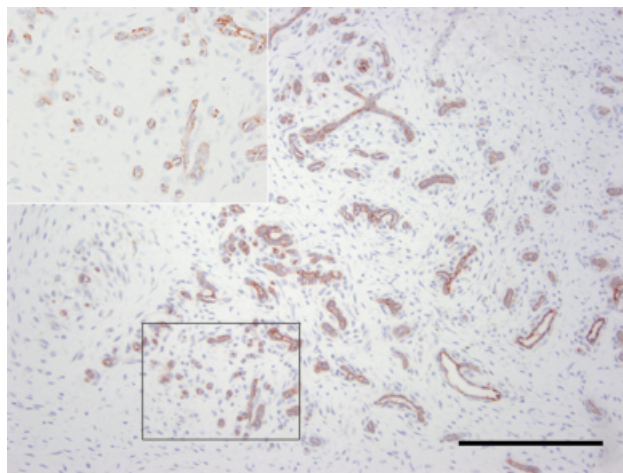


FIG. 5. Photomicrograph of formalin fixed deep digital flexor tendon with immunohistochemical staining for CD31. Notice the extensive staining, characteristic of a large number of small, endothelial lined vessels. Inset: Higher magnification of region outlined by black box. Hematoxylin counterstain; scale bar = 200  $\mu$ m.

tissue attenuation secondary to an increase in the tissue or blood vessel iodine concentration.

In the dynamic contrast-enhanced CT study, images were generated every other second for 90 s. In such a procedure, early contrast enhancement is consistent with an increase in blood flow while contrast retention is consistent with altered vascular permeability.<sup>24</sup> Although the characteristics of dynamic contrast-enhanced CT imaging in normal tendons are unknown, both increased flow and permeability were inferred based on similar studies in other organs. Furthermore, other more normal portions of the tendon within the same slice served as an internal control. Early, intense regional contrast enhancement representing increased blood flow and retention of contrast medium within the tendon lesion and the collateral sesamoidean ligament (approximately 30 s after regional venous contrast media clearance) was interpreted to represent increased permeability.

Achilles tendonopathy in humans has been assessed using contrast-enhanced MR imaging.<sup>18,21,23,27</sup> Early tendon enhancement was related to clinical signs of achillodynia. Increasing total enhancement, quantified as the area under the time vs. MR signal curve, was associated with increasing lesion severity.<sup>21</sup> Furthermore, contrast medium-enhanced T1-weighted MR images were the best sequence for identification of intratendinous lesions.<sup>21,23,27</sup> Contrast medium-enhanced T1-weighted images generally allowed identification of a larger abnormal region than routine T1-weighted images. Similarly, although quantification of lesion size was not performed, the contrast-enhanced images did give an impression of increased size.

The contrast medium injection technique used in previous CT studies is different than the approach used herein that involved a direct regional arterial injection vs. systemic

venous injection. Intraarterial injection may allow for greater accuracy in lesion characterization in patients with large body mass, such as horses.

The deep digital flexor tendon lesions were depicted similarly on MR and CT imaging, with good correlation with gross findings. Contrast-enhanced CT resulted in increased lesion conspicuity, particularly of the dorsal border lesion of the lateral lobe. This is similar to reports in humans.<sup>21,23,27</sup> Increased lesion conspicuity, secondary to increased tissue iodine, is likely the result of both increased permeability, as expected in the acute and subacute phases of tendon healing, and also increased blood flow through new vessel formation, as confirmed histopathologically using immunohistochemical staining for CD31, an endothelial cell marker.

New vessel formation and increased vascular permeability are important aspects of tendon injury and repair.<sup>16</sup> Conversely, increased tendon vascularization has been implicated in tendonopathy, without discreet tendon tearing,

and is associated with tendon pain in humans<sup>16–20</sup> and lameness, the technique of contrast-enhanced CT may be useful to further investigate this relationship. Currently, power flow Doppler techniques are advocated as a means of more thorough evaluating tendons through the identification of tendon hyperemia in humans and in equine superficial digital flexor tendons.<sup>17,19,20</sup> This technique will only be useful in tendons that are accessible to ultrasound interrogation and because of the hoof capsule and curvature of the distal deep digital flexor tendon, sonographic evaluation of this region remains commonly unattainable.

This horse represents a sentinel patient whereby the clinical utility of contrast-enhanced CT is documented and confirmed with pathology. Contrast-enhanced CT allowed identification of lesions that had good correlation with high field MR images and which were confirmed after euthanasia. The comparative value of CT vs. MR imaging of the distal extremity of the horse is unknown and further comparisons are needed.

#### REFERENCES

1. USDA, APHIS, VS. Lameness and laminitis in U.S. horses. Fort Collins, CO: Animal Health Monitoring System, 2000.
2. Stashak T. Adam's lameness in horses, 5th ed. Philadelphia: Lippincott, Williams and Wilkins, 2002.
3. Dyson S. Primary lesions of the deep digital flexor tendon within the hoof capsule. In: Ross M, Dyson S (eds): Diagnosis and management of lameness in the horse. St. Louis: Saunders, 2002;305–309.
4. Grewal JS, McClure SR, Booth LC, Evans RB, Caston SS. Assessment of the ultrasonographic characteristics of the podotrochlear apparatus in clinically normal horses and horses with navicular syndrome. *J Am Vet Med Assoc* 2004;225:1881–1888.
5. Murray RC, Blunden TS, Schramme MC, Dyson SJ. How does magnetic resonance imaging represent histologic findings in the equine digit? *Vet Radiol Ultrasound* 2006;47:17–31.
6. Dyson SJ, Murray R, Schramme MC. Lameness associated with foot pain: results of magnetic resonance imaging in 199 horses (January 2001–December 2003) and response to treatment. *Equine Vet J* 2005;37:113–121.
7. Dyson SJ, Murray R, Schramme M, Branch M. Collateral desmitis of the distal interphalangeal joint in 18 horses (2001–2002). *Equine Vet J* 2004;36:160–166.
8. Dyson S, Murray R, Schramme M, Branch M. Lameness in 46 horses associated with deep digital flexor tendonitis in the digit: diagnosis confirmed with magnetic resonance imaging. *Equine Vet J* 2003;35:681–690.
9. Blunden A, Dyson S, Murray R, Schramme M. Histopathology in horses with chronic palmar foot pain and age-matched controls. Part 1: navicular bone and related structures. *Equine Vet J* 2006;38:15–22.
10. Blunden A, Dyson S, Murray R, Schramme M. Histopathology in horses with chronic palmar foot pain and age-matched controls. Part 2: the deep digital flexor tendon. *Equine Vet J* 2006;38:23–27.
11. Widmer WR, Buckwalter KA, Fessler JF, Hill MA, VanSickle DC, Ivancevich S. Use of radiography, computed tomography and magnetic resonance imaging for evaluation of navicular syndrome in the horse. *Vet Radiol Ultrasound* 2000;41:108–116.
12. Whitton RC, Buckley C, Donovan T, Wales AD, Dennis R. The diagnosis of lameness associated with distal limb pathology in a horse: a comparison of radiography, computed tomography and magnetic resonance imaging. *Vet J* 1998;155:223–229.
13. Tietje S, Nowak M, Petzoldt S, Weiler H. Computed tomographic evaluation of the distal aspect of the deep digital flexor tendon in horses. *Pferdheilkunde* 2001;17:21–29.
14. Puchalski SM, Snyder JR, Hornof WJ, Macdonald MH, Galuppo LD. Contrast enhanced computed tomography of the equine distal extremity. In: American association of equine practitioners. Seattle, WA: AAEP, 2005.
15. Puchalski SM, Galuppo LD, Hornof WJ, Wisner ER. Intraarterial contrast-enhanced computed tomography of the equine distal extremity. *Vet Radiol Ultrasound* 2007;48:21–29.
16. Sharma P, Maffulli N. Tendon injury and tendinopathy: healing and repair. *J Bone Jt Surg* 2005;87:187–202.
17. Weinberg E, Adams M, Hollenberg G. Color Doppler sonography of patellar tendinosis. *Am J of Roentgenol* 1998;171:743–744.
18. Richards PJ, Dheer AK, McCall IM. Achilles tendon (TA) size and power Doppler ultrasound (PD) changes compared to MRI: a preliminary observational study. *Clin Radiol* 2001;56:843–850.
19. Newman JS, Adler RS, Bude RO, Rubin JM. Detection of soft tissue hyperemia: value of power Doppler sonography. *Am J of Roentgenol* 1994;163:385–389.
20. Kristoffersen M, Ohberg L, Johnston C, Alfredson H. Neovascularisation in chronic tendon injuries detected with colour Doppler ultrasound in horse and man: implications for research and treatment. *Knee Surg Sports Traumatol Arthrosc* 2005;13:505–508.
21. Shalabi A, Kristoffersen-Wiberg M, Papadogiannakis N, Aspelin P, Movin T. Dynamic contrast-enhanced MR imaging and histopathology in chronic achilles tendinosis. A longitudinal MR study of 15 patients. *Acta Radiol* 2002;43:198–206.
22. Navon G, Eliav U, Demco DE, Blumich B. Study of order and dynamic processes in tendon by NMR and MRI. *J Magn Reson Imaging* 2007;25:362–380.
23. Shalabi A, Kristoffersen-Wiberg M, Aspelin P, Movin T. MR evaluation of chronic Achilles tendinosis. A longitudinal study of 15 patients preoperatively and two years postoperatively. *Acta Radiol* 2001;42:269–276.
24. Dawson P. Functional imaging in CT. *Eur J Radiol* 2006;60:331–340.
25. Dawson P. Dynamic contrast-enhanced functional imaging with multi-slice CT. *Acad Radiol* 2002;9(Suppl 2):S368–S370.
26. Pollard RE, Gracia TC, Stieger SM, Ferrara KW, Sadlowski AR, Wisner ER. Quantitative evaluation of perfusion and permeability of peripheral tumors using contrast-enhanced computed tomography. *Invest Radiol* 2004;39:340–349.
27. Movin T, Kristoffersen-Wiberg M, Shalabi A, Gad A, Aspelin P, Rolf C. Intratendinous alterations as imaged by ultrasound and contrast medium-enhanced magnetic resonance in chronic achillogdynia. *Foot Ankle Int* 1998;19:311–317.